

Sulfur poisoning of the CO adsorption on Co(0001)

K. Habermehl-Ćwirzeń¹, J. Lahtinen*

Laboratory of Physics, Helsinki University of Technology, P.O. Box 1100, FIN-02150 HUT, Finland

Received 11 June 2004

Available online 2 October 2004

Abstract

CO adsorption on a sulfur covered cobalt surface at 185 K has been studied using XPS, TDS, LEED, and WF measurements. As in the case of CO adsorption on the clean Co(0001) surface, CO adsorbs and desorbs molecularly and no dissociation was observed. The saturation coverage of CO decreases linearly from 0.54 ML to 0.27 ML when the S pre-coverage increases to 0.25 ML. The WF increased during CO adsorption, but did not reach the value obtained for CO adsorption on the clean surface. The smaller work function change is explained by the reduced adsorption of CO on the sulfur-precovered surface. A reduction in the activation energy of desorption for CO from 113 kJ/mol to 88 kJ/mol was observed indicating weaker bonding of the CO molecules to the surface. The behavior of the CO/S/Co(0001) system was explained by a combination of steric and electronic effects.

© 2004 Elsevier B.V. All rights reserved.

Keywords: Carbon monoxide; Cobalt; Low energy electron diffraction (LEED); Low index single crystal surfaces; Sulphur; Thermal desorption spectroscopy; X-ray photoelectron spectroscopy; Work function measurements

1. Introduction

The interaction of CO with sulfur on transition metal surfaces is important in understanding the roles of poisons in heterogeneous catalytic processes. On one hand, sulfur is a common unwanted

component in the feed of the new CO-containing reactants like gasified biomass and methanol, both gaining attention as ecological alternatives in the energy and fuel sector, and on the other hand, CoMo catalysts are industrially used for hydrodesulfurization [1]. We consider cobalt based catalysts promising and inexpensive replacements for more noble palladium or ruthenium catalysts.

The adsorption of CO on sulfur pre-covered transition metal surfaces is not completely understood. Although blocking of CO adsorption and decreasing of the adsorption energy has been seen

* Corresponding author.

E-mail address: jouko.lahtinen@hut.fi (J. Lahtinen).

¹ Also: Department of Material Science, Darmstadt University of Technology, Petersenstr. 23, D-64287 Darmstadt, Germany.

in several cases, the mechanism by which the blocking takes place is still somewhat open. Pure site-blocking (steric effects) have been claimed e.g. on Pd(100) [2,3] and Fe(100) [4,5] surfaces but significant contributions from electronic interaction has been reported on Ni(100) [6–11], Ni(111) [12,13], Pt(111) [14–16] and Rh(111) [17] surfaces.

Most of the studies in the literature deal with adsorption of CO on S pre-covered nickel surfaces. On Ni(111) two sulfur structures has been reported, $p(2 \times 2)$ -S and $(\sqrt{3} \times \sqrt{3})R30^\circ$ -S. In the first one sulfur adsorbs at three-fold hollow sites. In the co-adsorbed layer the CO molecule is located at the on-top site in the vicinity of the S atom, which draws charge from the metal normally used for back-donation to CO. This results in decreased CO adsorption energy. The influence of S is local and affects about 6 Ni sites per one S atom [12].

On Ni(100) the CO coverage is mainly affected by steric effects, but the decrease in the activation energy for desorption can best be explained by short range electrostatic effects. Long range electronic effects were not excluded [6–8]. The S atoms are located at the four-fold hollow sites and they push the CO molecules from the on-top sites of clean Ni(100) into e.g. four-fold hollow sites featuring lower activation energy for desorption [9].

On Pt(111) surface, sulfur forms $p(2 \times 2)$ -S and $(\sqrt{3} \times \sqrt{3})R30^\circ$ -S structures and in the latter the S adsorption site is fcc [14,15]. Sulfur is claimed to remain on its adsorption site also during co-adsorption and thus the CO molecules are adsorbed between the S atoms at on-top sites and hollow sites [15]. It has also been shown that the $p(2 \times 2)$ -sulfur layer is compressed by the CO adsorption featuring S atom diffusion on the surface due to the repulsive CO–S interaction [14]. The activation energy for desorption decreases from about 120 kJ/mol to 60 kJ/mol due to Sulfur [15]. The continuous decrease in the desorption temperature of CO due to the increased S coverage seen on Pt(poly) suggests a long-range electronic interaction between the adsorbates according to Thomas et al. [16].

On Rh(111), the density functional calculations indicate that the local adsorption structures of CO

molecules and S atoms remain the same as obtained in the case of pure CO or S adsorption. The adsorption of S does not affect the chemisorption energy and this all suggest that there only is a short-range interaction between the adsorbates [17].

On cobalt surfaces, the effect of sulfur on the hydrogen adsorption has been studied [18]. The work function (WF) showed only a slight increase due to sulfur adsorption, resulting in 0.2 eV higher values for saturation S coverage. Increased sulfur coverage leads to a decreased adsorption of hydrogen, resulting in a complete blocking of hydrogen adsorption at sulfur saturation coverage.

In this work, we have studied the effect of sulfur on the CO adsorption on Co(0001) surface. This system was studied by XPS (X-ray Photoelectron Spectroscopy), TDS (Thermal Desorption Spectroscopy) and WF (Work Function) as well as LEED (Low Energy Electron Diffraction) measurements.

2. Experimental

All experiments were carried out in a stainless steel chamber, equipped with facilities for TDS, LEED, and XPS measurements. The UHV conditions were maintained by pumping the chamber with a combination of turbo molecular pump, ion pump, and titanium sublimation pump. The base pressure in the chamber was less than 2×10^{-10} Torr.

The feasible temperature for the measurements ranged between 160 and 690 K. The lower temperature was restricted by the cooling system, the upper by the phase transformation of cobalt from hcp to fcc.

The sample was a 11 mm diameter Co(0001) single crystal. The cobalt sample was mounted on the sample holder by spot-welded tantalum wires. These wires were also used for conducting the heating current to the sample. The detailed experimental set-up and initial cleaning procedure of the cobalt crystal has been given in [19–21]. The initial cleaning process left the sample in such a good condition that argon sputtering and annealing before each experiment was enough to obtain

an atomically clean surface. XPS and LEED were used to verify the cleanliness.

As a sulfur source, we used H₂S (AGA 99.8%). The H₂S exposure was given at 200 K sample temperature using a leak valve and a small tube guiding the gas directly onto the sample. After that H₂S was thermally decomposed on the sample surface at 650 K and hydrogen desorption was detected. The amount of sulfur was then measured with XPS. The CO (AGA 99.997%) was conventionally dosed using a leak valve. Both CO and H₂S were used as received.

The saturation coverage of sulfur at 200 K was determined to 0.25 ML² using the saturation of the S2p XPS line combined with a clear $p(2 \times 2)$ LEED pattern visible slightly before and at the saturation coverage. The sulfur coverage after individual exposures was then obtained by comparing the 2p XPS intensities against the saturation curve.

The XPS measurements were performed using a bias voltage of -25 V at the sample. This procedure insured that the photoelectron signal was originating from the sample only.

3. Results

Adsorption of CO on the sulfur covered Co(0001) surface was performed at 180 K. The coverage range of sulfur extended from zero up to 0.25 ML. Carbon monoxide exposures of 1, 2, and 10 L were chosen, as these resemble well different stages of the CO adsorption on clean Co(0001). The maximum exposure of 10 L was sufficient to saturate all surfaces.

With LEED, two different co-adsorption structures were seen as shown in Fig. 1. Plain sulfur exhibits a $p(2 \times 2)$ structure that is at best with $\theta_s = 0.25$ ML, and CO exposures below 2 L did not change the LEED pattern. Upon increased CO exposures, the LEED pattern changed to feature the $(2\sqrt{3} \times 2\sqrt{3})R30^\circ$ symmetry. This corresponds to the saturation CO exposure.

3.1. XPS studies

The C1s spectra for CO exposures of 1 L and 10 L for the clean cobalt surface, and with sulfur coverage of 0.11 ML and 0.25 ML are shown in Fig. 2. The peaks are observed to decrease after both CO exposures as the sulfur coverage increases. This indicates blocking of adsorption sites.

For zero sulfur coverage and CO exposures of 1 L and 2 L, (not shown) the spectra were fitted with a single peak at 286.4 eV. As the CO exposure increased, a second component at 285.8 eV became necessary. This repeats our previous results on clean Co(0001) [22]. The component at the higher binding energy indicates on-top adsorption while the lower BE component corresponds to adsorption at bridge or hollow sites featuring also lower activation energy for desorption in our earlier study [22]. When the sulfur coverage increases, both components were needed to fit the C1s data.

The XPS measurements were repeated after CO desorption. No remaining carbon nor any loss in the sulfur intensity (not shown) was detected. Also the S2p peak remained at the same position as before desorption. This indicates that the S-atoms stay on the surface and most likely co-adsorbed CO did not affect the sulfur adsorption site.

3.2. Work function studies

The adsorption of sulfur increases the WF linearly on Co(0001) up to 0.2 eV at 0.25 ML of S. This is shown in the inset of Fig. 3. The initial dipole moment of the sulfur layer is -0.12 D if calculated using the Helmholtz equation.

We measured the change in the WF as a function of CO exposure for various S coverages and the results are shown in Fig. 3. The WF change due to sulfur adsorption has been subtracted from the WF curves to give a common zero for 0 L of CO.

3.3. Thermal desorption studies

During TDS only molecular CO desorption was observed. No reaction nor any decomposition products were obtained. In addition, XPS showed no remaining carbon on the surface, neither as

² One monolayer (ML) coverage is defined here as the number of adsorbates per number of surface atoms.

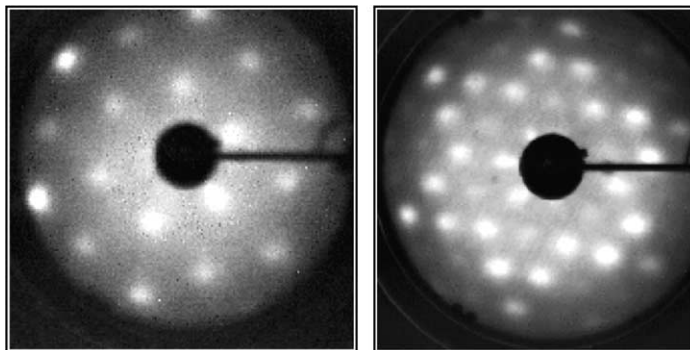


Fig. 1. Ordered LEED patterns on Co(0001). Left: the $p(2 \times 2)$ seen at brightest with S coverage of 0.25 ML with less than 2L of CO exposed; Right: the $(2\sqrt{3} \times 2\sqrt{3})R30^\circ$ structure seen with saturation CO exposure.

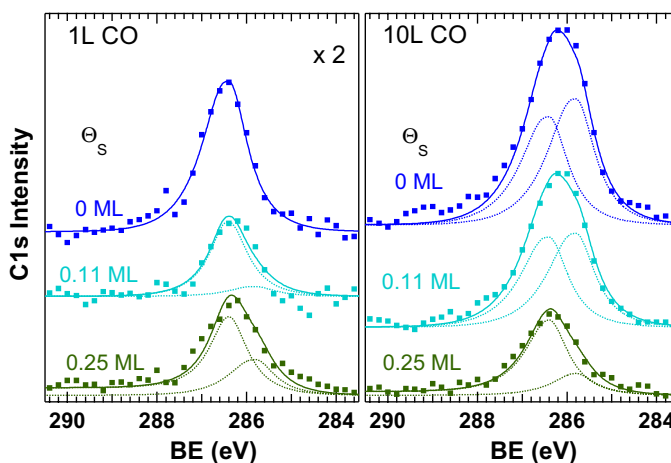


Fig. 2. Set of C1s data for 1L and 10L CO exposures on Co(0001) with different sulfur coverages. The intensity scale is same for both figures but the data in the 1L figure is multiplied by a factor of two. The spectra were fitted with two components at 286.4 eV and 285.8 eV shown with dotted lines. The solid line represent the sum spectra.

molecules nor as atomic carbon. This suggests that sulfur is neither promoting CO dissociation nor its disproportionation.

For 1L CO exposure on clean cobalt a single desorption peak at 400 K is present as seen in Fig. 4. With increasing exposures (2L and 10L), the peak area increases and several components appear in the main peak. Additionally, a second peak appeared on the low temperature side with a desorption maximum around 280 K. These data agree with the previously reported values on Co(0001) in [22].

Sulfur adsorption made the CO peaks shift to lower desorption temperatures with all CO

exposures. Fig. 4 indicates that both desorption peaks shift and decrease in intensity as the sulfur coverage increases. For sulfur coverage of 0.11 ML, the high temperature peak maximum is only slightly shifted at 390 K but the low temperature peak maximum at 260 K shows a shift of 20 K. At sulfur saturation, the lower temperature peak has more clearly moved down in temperature about 40–240 K and the high temperature peak shifted about 85–315 K.

The CO activation energy for desorption after 10L of CO was significantly reduced due to the sulfur. Using the Redhead formula [23] for first order desorption with a frequency factor of 10^{13} s^{-1} ,

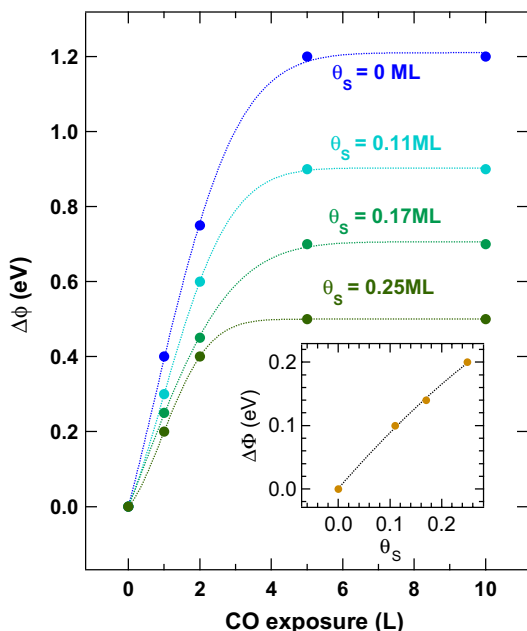


Fig. 3. Work function change as a function of CO exposure for various amounts of S on the surface. The values corresponding to 0L CO exposure is adjusted to 0eV in each case. The evolution of this offset as a function of S coverage is shown in the inset.

the activation energies for desorption for the high temperature peak were estimated to 113 ± 2 kJ/mol, 111 ± 2 kJ/mol, and 88 ± 1 kJ/mol for sulfur coverage of 0, 0.11, and 0.25 ML, respectively. The low temperature peak showed activation energies of 78 ± 1 kJ/mol, 73 ± 1 kJ/mol, and 66 ± 1 kJ/mol for the above sulfur coverages.

4. Discussion

4.1. On the adsorption site

The carbon monoxide coverage as a function of the sulfur coverage is depicted in Fig. 5. The filled circles and squares represent data obtained from C1s peak areas of Fig. 2 for 1L and 2L (bottom), and 10L (top) CO exposure as a function of the sulfur coverage. The coverage calibration was done based on the CO saturation coverage of 0.54 ML on clean Co(0001) at 180 K [22]. The open markers in Fig. 5 are obtained by integrating

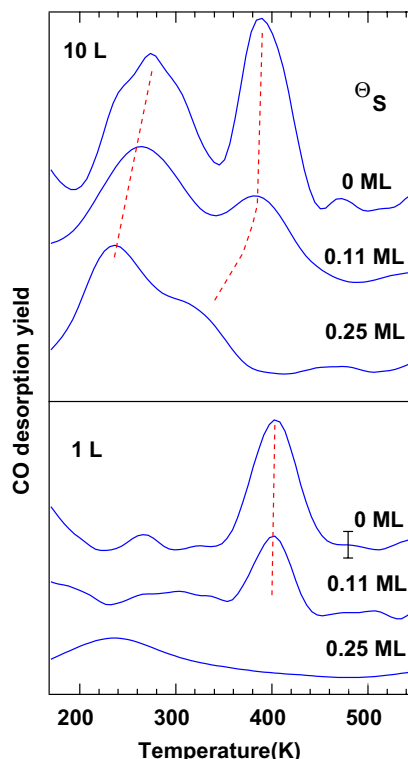


Fig. 4. Two sets of TDS data for CO exposures of 1 L and 10 L for three different sulfur coverages. Noise from the original data has been smoothed using a noise level indicated with the error bar on the 0 ML of S + 1 L of CO curve.

the desorption spectra of Fig. 4 using the same saturation coverage as with the XPS data. The triangles represent work function change values from Fig. 3 but in this case, the work function maximum on the right hand scale is adjusted to give the same marker location at zero S coverage as the XPS and TDS data sets.

All the data points in Fig. 5 fall nicely on the same slope indicating direct blocking of CO adsorption sites. From the saturation (10 L) CO exposure data we get one sulfur atom blocking effectively 1.2 CO sites. Similar linear coverage dependence has been seen with Ni(111), where one S atom blocks 2.1 CO sites [12], on Ni(100) where one S atom blocks 1.4 CO sites [7] or about 10 Ni sites [11]. On Pd(100) surface the blocking is not linear and more efficient with small S coverage [2,3].

It should be noted that a complete blocking of adsorption—found in the case of H₂ adsorption

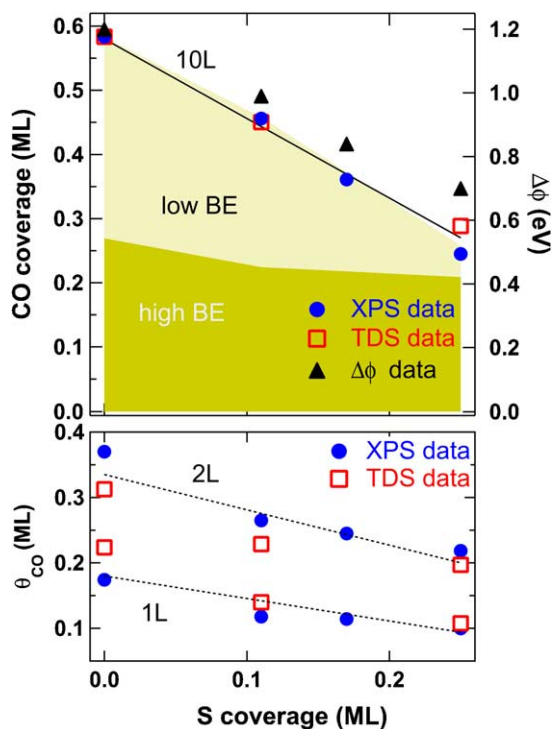


Fig. 5. The amount of adsorbed CO on Co(0001) as a function of sulfur coverage for CO exposures of 1L and 2L (below) and 10L (above). The solid symbols refer to XPS data and the open symbols to the TDS data. The filling refers to the area of the two components used in the fitting of the C1s line. The triangles refer to the work function change on the right hand scale.

on Co(0001) [18]—is not seen with CO. Saturation coverage of sulfur only leads to a reduction in the adsorption of CO. We assume that the reason for the different behavior lies in the dissociative adsorption of H₂ requiring two adjacent adsorption sites.

In Fig. 5, the coverages of the low (light filling) and high (dark filling) BE component from Fig. 2 are shown for 10L CO exposure. The data suggests that the adsorption at the high BE state is only slightly modified by sulfur whereas the adsorption on the low BE state is strongly reduced. This leads us to propose the following: the high BE is reported to correspond to adsorption at on-top sites on clean Co(0001) [22] and thus we assume the CO molecules to adsorb mainly at the on-top

sites also with 0.25 ML of sulfur. From the TDS data we observe that the desorption peaks shift down in temperature. Assuming on-top site for CO leads us to propose a decreased binding of CO molecules to the surface and an electronic effect in the S–CO interaction.

The proposed on-top adsorption site for CO indicates because of symmetry that the S atoms adsorb on the three-fold hollow sites. This is in line with the S adsorption at four-fold hollow site on fcc cobalt [24], at the fcc sites on Ni(111)-(2×2)-S [25], and on Pt(111)-(√3×√3)R30°-S [26] structures. On Pt(111), sulfur is claimed to stay on the fcc sites also during co-adsorption [15].

In the case of (2×2)-(S + CO) structure the surface is definitely dominated by sulfur but the adsorption of CO is still possible. The (2×2) structure was seen below 2L CO exposures corresponding to CO coverages below 0.2 ML. The adsorption site for CO is assumed to be “on-top” but based on the appearance of the low BE peak in the C1s data with small CO exposure and 0.25 ML of sulfur the S atoms seem to push a fraction of the CO molecules from the preferential on-top sites to hollow sites. This low exposure data suggests an interaction distance that is larger than the blocking ability of one S atom. The suggested structure is drawn in Fig. 6 but here the CO coverage is 0.25 ML if all the CO sites are occupied.

The (2√3×2√3)R30° structure corresponds to sulfur coverage of 0.25 ML and CO coverage of 0.3 ML. The suggested structure is drawn in Fig. 6. The S–CO interaction is assumed to move the CO molecules slightly from the on-top sites while the S atoms are still located at the hollow sites. The additional CO molecules (one out of four) are adsorbed at the three-fold hollow sites in accordance with the intensity of the low BE peak after 10L of CO. The constant adsorption site for sulfur is supported by the S2p peak remaining at the same position during all the experiments. The total surface coverage 7/12 in this structure is the same as observed with saturation of pure CO adsorption on Co(0001) [22], indicating that there are a maximum number of allowed dipoles per surface area. This latter structure resembles the one suggested by Kelemen et al. for Pt(111),

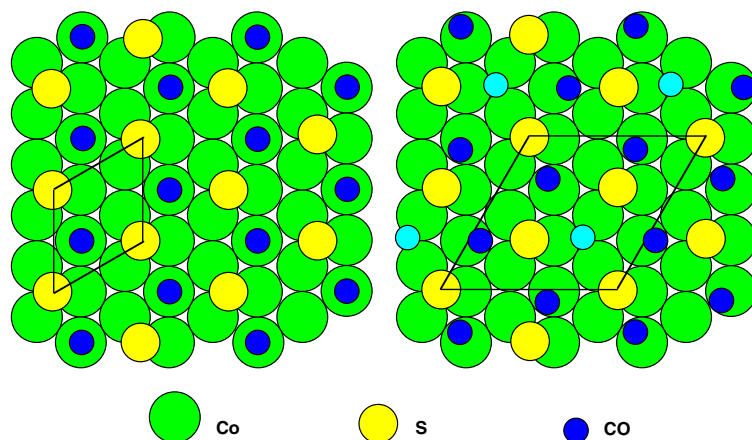


Fig. 6. The proposed surface structures corresponding to the (2×2) -S + CO (left) and $(2\sqrt{3} \times 2\sqrt{3})R30^\circ$ -(3S + 4CO) (right) structures on Co(0001). The sizes of the circles correspond approximately to the covalent radii of Co, C and S atoms.

although in their model two different adsorption sites for CO were observed [15].

4.2. On the interaction

The changes in the work function due to pure CO adsorption on Co(0001) have been studied earlier [22]. CO adsorption increased the work function by 1.2 eV for the saturation coverage. This yielded, an initial dipole moment of -0.32 D. The initial dipole moment for the S layer was -0.12 D, which is smaller than the value -0.26 D observed on the Ni(100) surface [7]. The difference is mainly due to the close packing of the Co(0001) surface.

The presence of sulfur leads to a smaller value of the saturation change in the work function. The reason can be seen in Fig. 5, where the coverage - determined with XPS—is combined with the TDS data and the work function change, and the same slope for all curves is observed. This indicates that the main effect of S on the surface is blocking of the CO adsorption sites.

If we calculate the work function change due to the co-adsorbed layer using the initial dipole moments for S and CO in the case of saturation exposures, we get a value $\Delta\phi = 0.76$ eV. This is only slightly larger than the experimental value 0.7 eV

indicating that mutual depolarization between these adsorbates is rather small.

The thermal desorption data shows gradual decline in the activation energy for desorption with increasing S coverage. A continuous reduction in the thermal desorption temperature indicates long-range interactions between sulfur and carbon monoxide as suggested on Pt by Thomas et al. [16]. In this work we observed a small decrease in the CO peak maximum due to small S coverage, whereas the desorption energy for the high temperature peak decreases by 25 kJ/mol from 113 kJ/mol when the S coverage increases from zero to 0.25 ML. Simultaneously with the downward shift the peak area decreases so that the main desorption component at 0.25 ML S coverage corresponds to desorption energy of 66 kJ/mol. This overall decrease is in line with previous studies; on Pd(100) the decrease was from 142 kJ/mol to 105 kJ/mol [2], on Pt(100) from 126 kJ/mol to 63 kJ/mol [15] and on Fe(100) from 90 kJ/mol to 45 kJ/mol [4], indicating a factor two in the change.

The decrease in the desorption energy is explained by the reduced back-donation to the CO molecule from the metal atom. This is caused by the closely located S atom attracting charge from the Co substrate used for CO back donation [12]. Our proposed model for the $(2\sqrt{3} \times$

$2\sqrt{3}R30^\circ$ structure features these close CO–S pairs.

5. Conclusions

We have studied the co-adsorption of S and CO on Co(0001) surface. The presence of sulfur on the cobalt surface does not lead to any new reaction products. Sulfur is bonded strongly to the cobalt surface and does not desorb during TDS. CO stays intact on the surface until it desorbs molecularly during heating. No atomic carbon or oxygen traces are found during or after the heating.

Our results indicate a combination of local and long-range interactions between sulfur and carbon monoxide as it was also suggested by Hardegree for Ni(100) [6] and by Thomas for platinum [16]. As found in other cases, sulfur blocks the adsorption of CO. The direct blocking of adsorption sites is evidenced by the ability of one S atom to block effectively 1.2 CO sites.

Sulfur caused a redistribution of CO adsorption sites on the surface. Two surface structures were suggested corresponding to the observed LEED structures. In the TDS a decrease in the activation energy for desorption was visible. Electronic effects are indicated by the continuous shift of the CO desorption peaks to lower temperatures as well as the electron acceptor behavior of both sulfur and carbon monoxide leading to an electronic modification of the of S/Co(0001) surface.

Acknowledgment

We acknowledge Mr. Aapo Varpula for his assistance during the measurements and Mr. Mikko Aronniemi for his help with the XPS data fitting. This work was supported by the Academy of Finland and the National Graduate School of Materials Physics.

References

- [1] H. Topsøe, B.S. Clausen, F.E. Massoth, in: J.R. Anderson, M. Boudart (Eds.), *Hydrotreating Catalysts Catal. Science Technol.*, vol. 11, Springer, Berlin, 1996.
- [2] T. Yamada, Z. Runsheng, Y. Iwasawa, K. Tamaru, *Surf. Sci.* 205 (1988) 82.
- [3] S.W. Jorgensen, R.J. Madix, *Surf. Sci.* 163 (1985) 19.
- [4] J. Benziger, R.J. Madix, *Surf. Sci.* 94 (1980) 119.
- [5] D.W. Moon, D.J. Dwyer, S.L. Bernasek, *Surf. Sci.* 163 (1985) 215.
- [6] E.L. Hardegree, P. Ho, J.M. White, *Surf. Sci.* 165 (1986) 488.
- [7] P. Ho, E.L. Hardegree, J.M. White, *Surf. Sci.* 165 (1986) 507.
- [8] J.L. Gland, R.J. Madix, R.W. McCabe, C. DeMaggio, *Surf. Sci.* 143 (1984) 46.
- [9] N. Vasquez, A. Muscat, R.J. Madix, *Surf. Sci.* 339 (1995) 29.
- [10] S. Johnson, R.J. Madix, *Surf. Sci.* 108 (1981) 77.
- [11] M. Kiskinova, D.W. Goodman, *Surf. Sci.* 108 (1981) 64.
- [12] M. Trenary, K.J. Uram, J.T. Yates Jr., *Surf. Sci.* 157 (1985) 512.
- [13] G.A. Sargent, G.B. Freeman, J.L.-R. Chao, *Surf. Sci.* 100 (1980) 342.
- [14] B.J. McIntyre, M. Salmeron, G.A. Somorjai, *Surf. Sci.* 323 (1995) 189.
- [15] S.R. Kelemen, I.E. Fischer, J.A. Schwarz, *Surf. Sci.* 81 (1979) 440.
- [16] V.D. Thomas, J.W. Schwank, J.L. Gland, *Surf. Sci.* 464 (2000) 153.
- [17] C.J. Zhang, P. Hu, M.-H. Lee, *Surf. Sci.* 432 (1999) 305.
- [18] K. Habermehl-Cwirzeń, K. Kauraala, J. Lahtinen, *Physica Scripta T108* (2004) 28.
- [19] J. Lahtinen, J. Vaari, A. Talo, A. Vehanen, P. Hautojärvi, *Surf. Sci.* 245 (1991) 244.
- [20] J. Lahtinen, J. Vaari, K. Kauraala, E.A. Soares, M.A. van Hove, *Surf. Sci.* 448 (2000) 269.
- [21] J. Vaari, J. Lahtinen, T. Vaara, P. Hautojärvi, *Surf. Sci.* 346 (1996) 1.
- [22] J. Lahtinen, J. Vaari, K. Kauraala, *Surf. Sci.* 418 (1998) 502.
- [23] P.A. Redhead, *Vacuum* 12 (1962) 203.
- [24] M. Maglietta, *Solid State Commun.* 43 (1982) 395.
- [25] J.E. Demuth, D.W. Jepsen, P.M. Marcus, *Phys. Rev. Lett.* 32 (1974) 1182.
- [26] K. Hayek, H. Glassl, A. Gutman, H. Leonhard, M. Prutton, S.P. Tear, M.R. Welton-Cook, *Surf. Sci.* 152 (1985) 419.